

The Novel biocatalytic cascade ZIF-8 capsule/Polysulfone Stereostructure and its Application in Amperometric Glucose Biosensors

Cang Wang¹, Min Pan¹, Hang Chen¹, Dajing Chen^{2,*}, Yuquan Chen^{1,*}

¹Department of Biomedical Engineering, Zhejiang University, Hangzhou 310027, China

²Medical School, Hangzhou Normal University, Hangzhou, 311121, China

*E-mail: djchen@hznu.edu.cn

Received: 7 May 2019 / Accepted: 21 June 2019 / Published: 31 July 2019

In this study, we present a novel zeolitic imidazolate framework-8 metal–organic framework/polysulfone (PSF) stereostructure with glucose oxidase (GOx) and horseradish peroxidase (HRP) encapsulated in ZIF-8 as nanoreactors. This work links the high biocatalytic activity and great stability of the enzymes encapsulated in ZIF-8 with the large surface area and mass transport of the three-dimensional microporous PSF and highlights the pore structure of PSF, which blocks cells during whole blood testing. The prepared ZIF-8 capsule/PSF structure exhibits a 1.2-fold and 2.4-fold increase in sensitivity compared with the ZIF-8 capsule powder and bulk mixture of GOx and HRP, respectively. The modified ZIF-8 capsule/PSF glucose biosensor exhibited a 0-18 mM linear range and good selectivity. Furthermore, the prepared sensor attenuated less than 10% after 50 replicate whole blood tests. These advanced properties give the novel biocatalytic cascade ZIF-8 capsule/polysulfone stereostructure promising applications in whole blood monitoring.

Keywords: ZIF-8; nanostructure; glucose oxidase; horseradish peroxidase; glucose biosensor.

1. INTRODUCTION

Blood glucose monitoring, as an important part of whole blood monitoring, is critically needed for the management of both type I and type II diabetes. Although disposable blood glucose detection strips are widely used, there is a considerable need for the development of whole blood detectable glucose biosensors with highly repeatability and a wide-linear-range[1, 2]. The microporous metal organic framework (MOF) represents one of the most promising materials in biosensors. In addition to its applications in gas storage and separation[3-5], substantial research has been directed towards the development of MOF carriers due to its controllable pore size and surface functionality[6-8]. Enzymes,

as important functional proteins, are popular substances that researchers want to load into MOFs[8-10]. Recently, Chen[11] capsulated a multienzyme system into ZIF-8 as a microcapsule reactor instead of using normal surface adsorption. The integration of this two-enzyme system (glucose oxidase, GOx and horseradish peroxidase, HRP) in ZIF-8 led to enhancements in the activity of the catalytic cascade. However, Chen discussed the ZIF-8 reactor as a powder but did not mention its applications in 3D structure.

Porous polysulfone (PSF) is a widely used porous polymer support that has flexible, asymmetric properties. The submicropores on the surface can easily separate red blood cells[12, 13]. Due to its organic character, a MOF can interact with PSF more easily than inorganic substrates. Different kinds of MOFs were synthesized on porous PSF supports, such as ZIF-8[14], ZIF-90[15] and Bio-MOF-1[16]. However, the porous structure of PSF with MOF loaded has mostly been used for gas separation or storage and has rarely been used as a filter membrane for blood.

In the present work, we report a novel ZIF-8 capsule/PSF stereostructure with GOx and HRP encapsulated in ZIF-8 and explore its applications as an amperometric glucose biosensor. The prepared ZIF-8 capsule/PSF structure exhibits higher sensitivity compared with the ZIF-8 capsule powder, and the modified ZIF-8 capsule/PSF glucose biosensor showed a great linear range and good selectivity. Furthermore, the prepared sensor showed great performance in the whole blood repeatability test. The results demonstrated that the novel biocatalytic cascade ZIF-8 capsule/polysulfone stereostructure has promising applications in whole blood monitoring.

2. EXPERIMENTAL

2.1 Reagents and equipment

All chemicals used were of analytical grade and were used as received without any further purification. Modified polysulfone (PSF) porous membranes were obtained from Harvest company as commercial products. The carbon slurry was purchased from the Acheson colloids company (Product: Electrodag 423SS). Glucose oxidase (GOx, EC 232-601-0, from *Aspergillus niger*) and horseradish peroxidase (HRP, RZ 2.9, from *horseradish*) were purchased from Aladdin. Glucose, glutaraldehyde (GA), zinc acetate ($\text{Zn}(\text{CH}_3\text{COO})_2$), 2-methylimidazole, paraffin wax, 2,2'-azino-bis(3-ethylbenzothiazoline-6-sulfonic acid) diammonium salt (ABTS), o-dianisidine, Nafion® 117 solution, sodium phosphate (Na_2HPO_4), sodium dihydrogen phosphate (NaH_2PO_4), sodium hydroxide (NaOH), ascorbic acid (AA), uric acid (UA) and ProClin 300 were supplied by Sigma-Aldrich (China). The supporting electrolyte used for the electrochemical studies was a 0.05 M phosphate buffer solution (PBS), prepared using Na_2HPO_4 and NaH_2PO_4 and adjusting the pH with either HCl or NaOH. The glucose solution was stored at 26°C for 24 h for mutarotation before use. Aqueous solutions were prepared in deionized water (DI). Fresh blood samples were provided from two healthy volunteers and two diabetic patients.

The precipitate of the experimental ZIF-8 was centrifuged with an Ohaus Frontier FC5816 laboratory centrifuge. The morphology of the ZIF-8 capsule/PSF was observed by field-emission scanning electron microscopy (SEM) (Hitachi SU8010). Crystal composition was identified by EDS and SEM mapping. Fourier transform infrared (FT-IR) spectra were recorded with an AVATAR 370

spectrophotometer between 4000 and 500 cm^{-1} . The crystalline structures of the samples were characterized by X-ray diffraction (XRD) via a Rigaku D/max 2400. The wavelength of the radiation source was 1.54 Å. The absorbance values were measured at 450 nm using a microplate reader (Multiskan FC, Thermo, Waltham, MA, USA). UV-Visible absorption spectra were collected using a double beam spectrophotometer (UV-2600, Shimadzu, Japan) with a 1 ml quartz cell. Amperometric measurements were performed using a CHI660E electrochemical workstation (Shanghai Chenhua, China) with a standard three-electrode system by applying a Ag/AgCl (1.0 M KCl) electrode and a platinum net (geometric area, 0.96 cm^2) as the reference and counter electrodes, respectively. The serum glucose analyses were conducted using a YSI 2300 STAT PLUS (Yellow Springs Instruments, Ohio, USA). An ultrasonic cleaner (JPS-80A, USA Lab) was used for the ultrasonic cleaning of the cells and proteins attached to the sensor's surface. All of the experiments were conducted at room temperature.

2.2 Synthesis of two-enzyme encapsulated ZIF-8 nanoparticles

Two-enzyme encapsulated ZIF-8 nanoparticles were prepared according to a previous report[11]. Typically, 1 ml of zinc acetate (20 mM) containing 100 μg GOx and 100 μg HRP was stirred gently at room temperature for 30 min. Afterwards, an equal volume of a 1.4 M 2-methylimidazole solution was quickly poured into the mixture and stirred with a magnetic stirrer for 30 min. Then, the obtained opaque solution was kept in an oven at 40°C for 30 min and centrifuged (5000 rpm, 10 min). The white sediment was filtered, washed thoroughly with deionized water, and dried in air for 24 h. For comparison, a similar ZIF-8 sediment was prepared without GOx and HRP using the same method.

2.3 Synthesis of ZIF-8 capsule/PSF stereostructure

Before the immobilization of the ZIF-8 capsule, hydrophilic porous PSF membranes were washed by immersion in deionized water for 24 h and dried overnight at room temperature.

For the synthesis of the ZIF-8 capsule in the porous PSF membranes, a self-assembling reaction was carried out as follows (Scheme, Fig. 1). (I) Two microliters of 5% GA solution was dropped and dried under air at room temperature for 30 min, and the resulting membrane was rinsed 3 times with deionized water and dried in a drying oven at 40°C for preparation. (II) The prepared membranes were soaked in a 20 mM $\text{Zn}(\text{CH}_3\text{COO})_2$ mixture solution containing 100 $\mu\text{g ml}^{-1}$ GOx and 100 $\mu\text{g ml}^{-1}$ HRP and bubbled with a peristaltic pump (100 rpm) for 15 min. Then, the treated membrane was gradually immersed into a 1.4 M 2-methylimidazole solution and bubbled with the pump (100 rpm) for 30 min. (III) After bubbling, the membrane was kept in an oven at 40°C for different times, from 5 min to 1 h. (IV) The obtained membrane was carefully washed 3-4 times with deionized water and then dried in air for 24 h.

2.4 Preparation of the modified biosensor

The prepared ZIF-8 capsule/PSF membrane was modified with 5% Nafion twice. To prepare the easily fabricated amperometric glucose biosensors, an appropriate amount of carbon slurry was brushed on the bottom surface of the membrane. After the carbon slurry dried overnight at room temperature,

paraffin was coated onto it to prevent direct contact with the solution. The biosensor was stored in the fridge at 4°C when not in use.

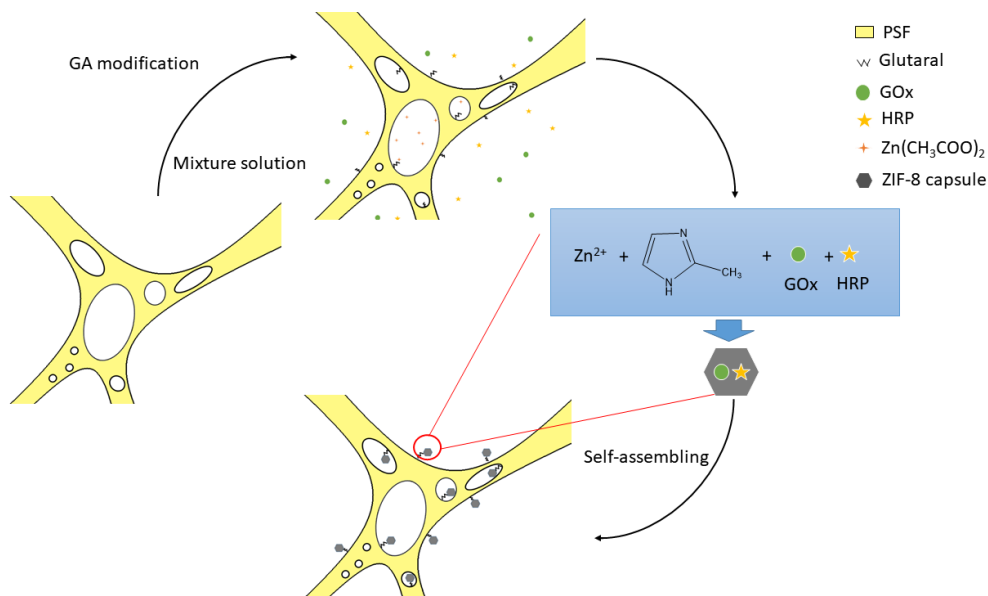


Figure 1. Schematic for the fabrication of the ZIF-8 capsule/PSF stereostructure membranes.

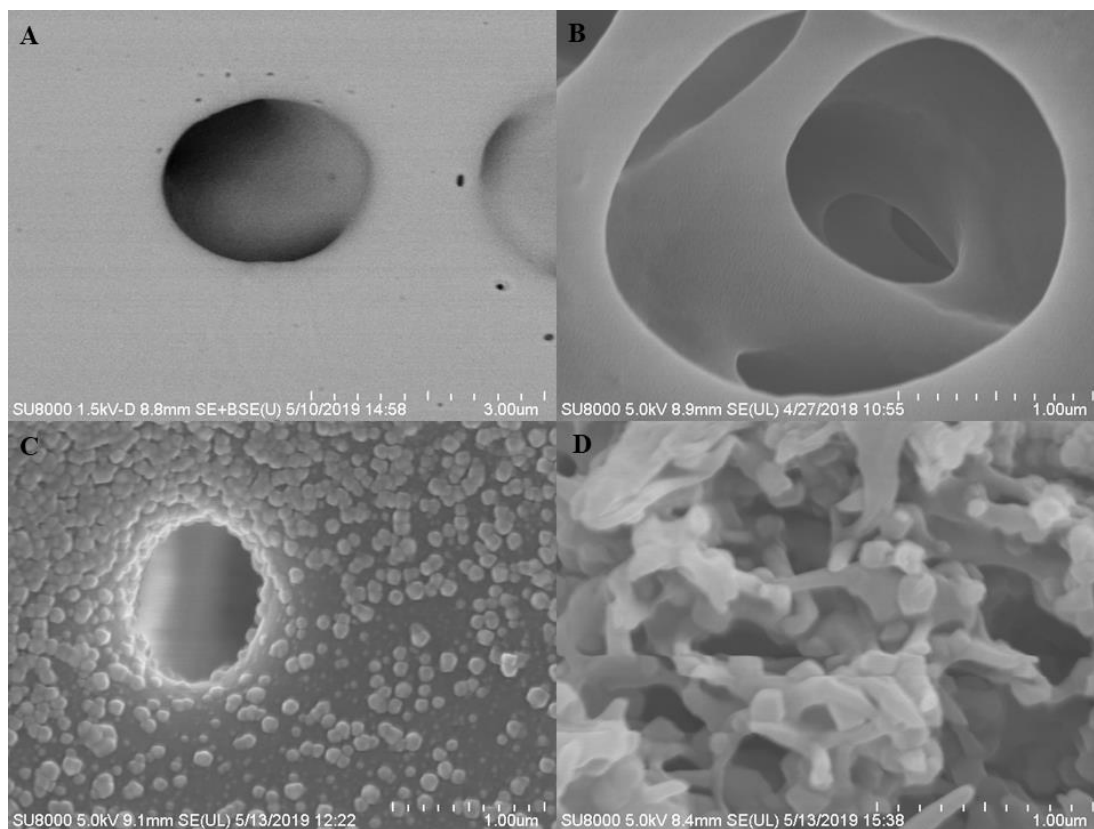
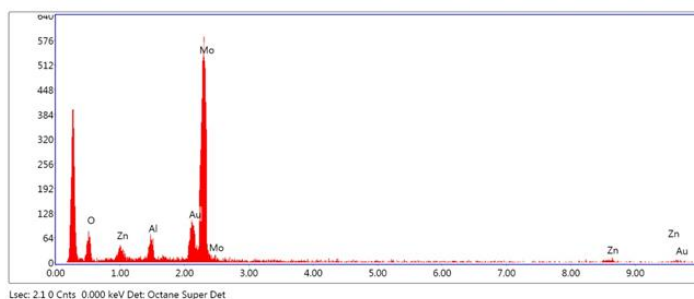
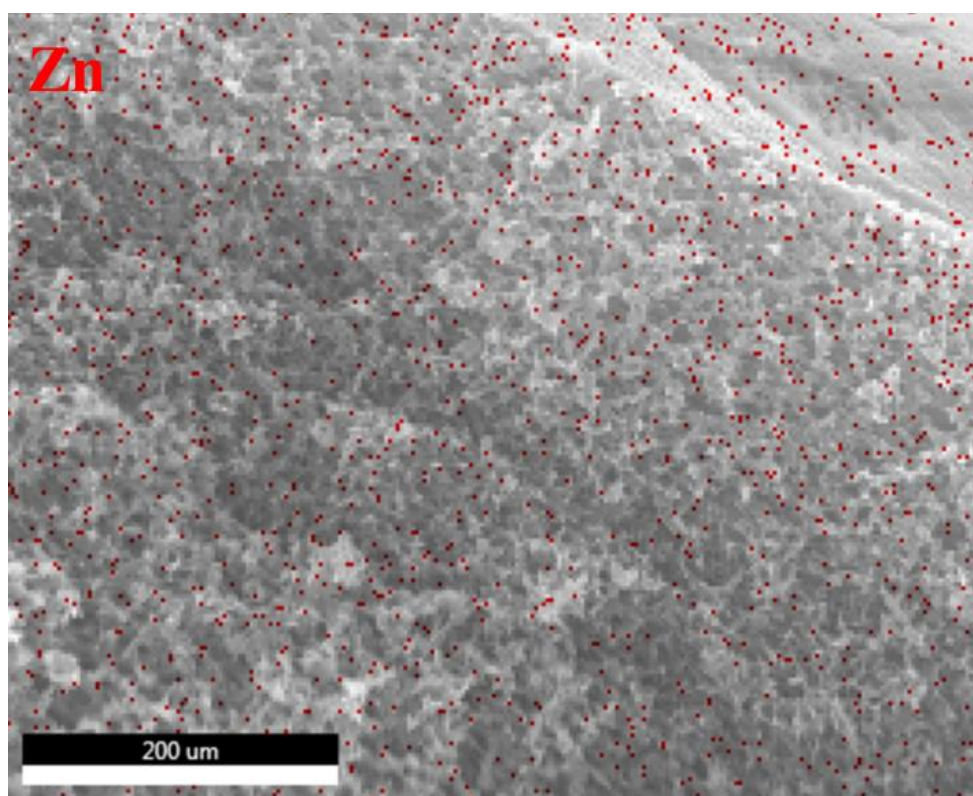


Figure 2. (A) Top view SEM image of the modified porous PSF membrane; (B) An enlarged image of the porous PSF membrane cross-section; (C) Top view image of the ZIF-8 capsule/PSF membrane; (D) An enlarged image of the ZIF-8 capsule/PSF membrane cross-section.



eZAF Smart Quant Results

Element	Weight %	Atomic %	Net Int.	Error %	Kratio	Z	R	A	F
O K	17.59	54.55	220.30	16.91	0.0349	1.3516	0.8210	0.1466	1.0000
AlK	2.97	5.47	201.10	13.90	0.0211	1.2062	0.8717	0.5866	1.0040
AuM	10.52	2.65	313.40	11.78	0.1026	0.7792	1.2089	1.1258	1.1105
MoL	61.93	32.03	2119.20	5.10	0.5362	0.9257	1.0532	0.9318	1.0037
ZnK	6.98	5.30	43.60	34.02	0.0757	1.0207	0.9932	0.9858	1.0785

Figure 3. SEM mapping image and EDS analysis of the ZIF-8 capsule/PSF membrane.

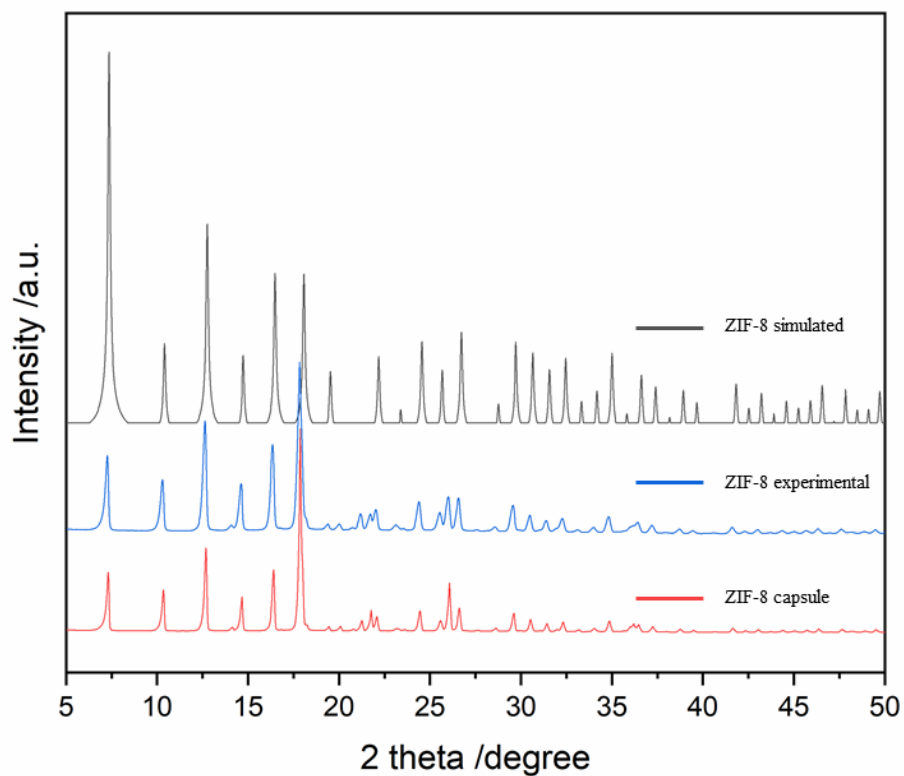


Figure 4. XRD spectra of simulated ZIF-8, experimental ZIF-8 and ZIF-8 capsules.

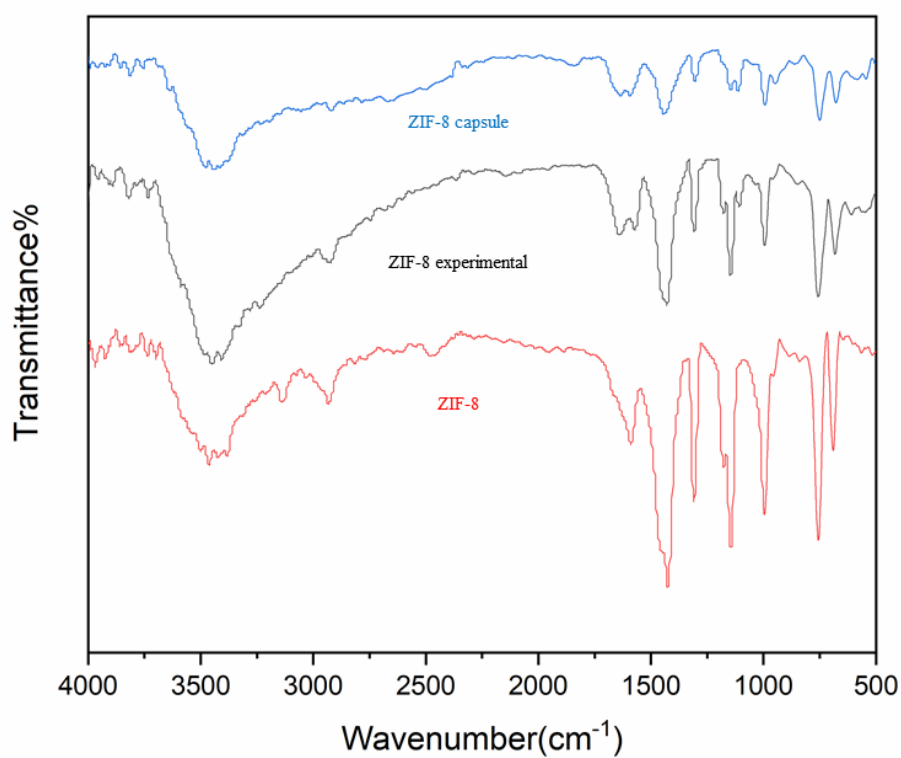


Figure 4. FT-IR spectra of simulated ZIF-8, experimental ZIF-8 and ZIF-8 capsules.

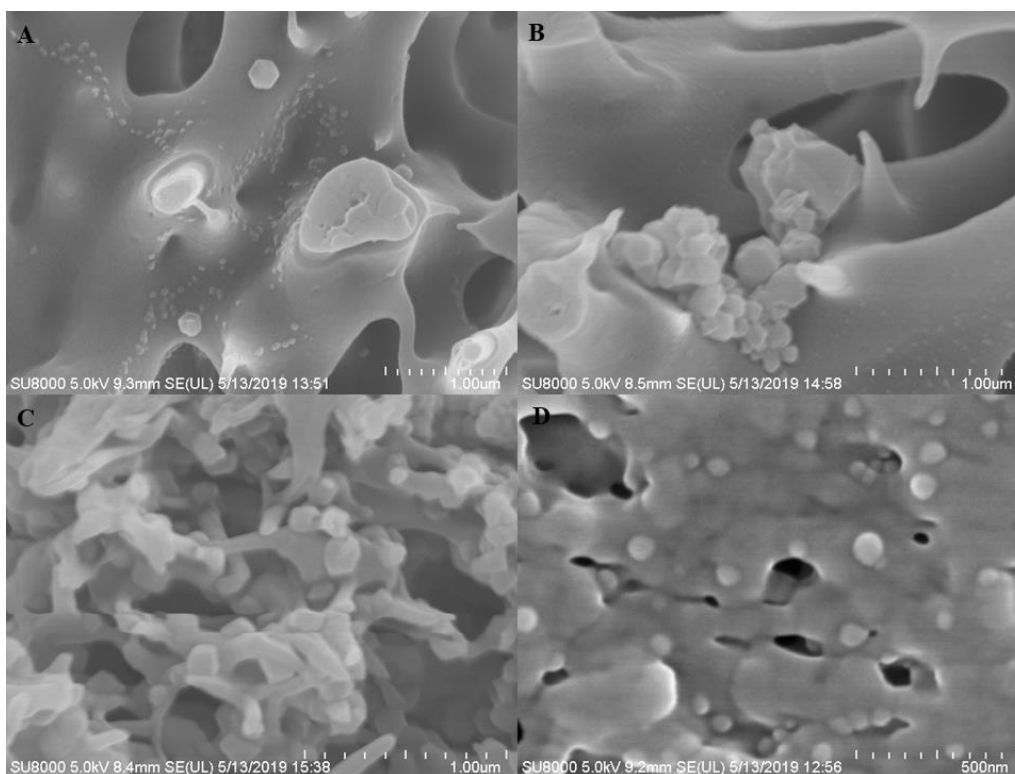


Figure 6. SEM images of ZIF-8 capsule/PSF membrane cross-section morphologies formed by the heating time of (A) 5 min, (B) 20 min, (C) 40 min, and (D) 1 h.

3. RESULTS AND DISCUSSION

3.1 Characterization of the ZIF-8 capsule/PSF stereostructure

Previously, different kinds of MOFs[17, 18] were immobilized in the three-dimensional macroporous matrix. Here, GOx/HRP enzymes encapsulated in ZIF-8 were immobilized in the PSF structure. Fig. 2C, D shows the SEM images of the ZIF-8 capsule/PSF stereostructure. The average size of the ZIF-8 capsule is 100 nm, as calculated with ImageJ software. Fig. 2A shows that the PSF film has a network-type morphology with microsized pores. Fig. 2B indicates that these micropores are interconnected, which could facilitate mass transport [19-21] and provide a large surface area for the reaction. Moreover, this cross-linked structure could also act as a filter blocking red blood cells with a diameter of 7 μm .

ZIF-8 capsules were formed in this PSF matrix through a spontaneous reaction between $\text{Zn}(\text{CH}_3\text{COO})_2$ and 2-methylimidazole with GOx and HRP confined, as Chen published[11]. Fig. 3A shows the SEM image of the modified PSF with SEM mapping. According to the SEM mapping picture, Zn was apportioned uniformly throughout the structure. As ZIF-8 was the only zinc source, this result demonstrates that ZIF-8 was evenly immobilized in the stereostructure. The EDS analysis and zinc concentration revealed that the film was composed of 6.98% wt Zn (Fig. 3B), which indicated that the mass ratio of the immobilized ZIF-8 capsule was approximately 24% wt.

XRD was used to study the crystalline structure of the synthesized particles. Fig. 4 shows the XRD spectra of experimental ZIF-8 and the ZIF-8 capsules in comparison with the simulated ZIF-8. Most of the characteristic diffraction peaks agree quite well with the simulated result in the database (information card for 602542) [4], indicating that the simulated ZIF-8, ZIF-8 capsule and comparison experimental ZIF-8 have a highly crystalline structure and an isostructural ZIF-8 framework. The small peaks observed at approximately 22 degrees and 25 degrees can be related to a change in crystallinity[22]. The peak at 17.8 degrees in each spectrum corresponds to the (0 1 3) plane, and the obvious shift of the peak to lower angles can be attributed to the enlarged interlayer spacing[23]. Evidently, this result suggested that the ZIF-8 capsules were successfully formed.

The FT-IR spectra of simulated ZIF-8, experimental ZIF-8 and ZIF-8 capsules in the range of 4000-500 cm^{-1} are presented in Fig. 5. Adsorption peaks at 1477 and 998 cm^{-1} are associated with the stretching and plane bending of the imidazole ring, respectively[24]. The strong band in the spectral region of 3000 cm^{-1} could be ascribed to the C-H, N-H and O-H stretching vibrations of the methyl, hydroxy and amine groups on the ZIF-8 nanoparticles[25].

Combining the SEM, EDS, XRD and FT-IR results (Figs. 2, 3, 4 and 5), a layer of well-dispersed ZIF-8 capsule particles became uniformly anchored in the PSF stereostructure instead of undergoing traditional bulk deposition. The average size of these particles was approximately 100 nm. During preparation, the GOx and HRP may have two functions. First, the GOx and HRP provide insufficient nucleation for the crystallization process to generate ZIF-8 capsules with a small size and improved dispersity. This result may be explained by the nonclassical seed-mediated growth theory[26]. This was confirmed by the fact that no obvious emulsion was formed without GOx and HRP in the precursor solution, and a milky solution formed as soon as GOx and HRP were added to the precursor solution. Second, the GOx and HRP biocatalytic cascade system can provide great selectivity and sensitivity to the prepared glucose sensors (Figs. 6-8).

3.2 Effects of heating time on ZIF-8 capsule generation

To optimize the formation of the ZIF-8 capsule layer, the membranes were produced with different heating times (ranging from 5 min to 1 h) as shown in Fig. 6. ZIF-8 starts with 50 nm particles, and 100 nm crystals were shown in Fig. 6A, which is relatively small for ZIF-8 particles (average 134-288 nm[27]). As the heating time increases, ZIF-8 particles grow and aggregate. Obvious ZIF-8 blocks can be found with a 20 min heating process (Fig. 6B). A ZIF-8 capsule layer with micropores was formed when the heating time increased to 40 min (Fig. 6C). With a 1 h heating process, the synthesized ZIF-8 layer almost blocked the whole PSF structure. This phenomenon proved that the heating time successfully controlled the aggregation of the ZIF-8 capsule and that the size of the synthesized ZIF-8 capsule particles remained relatively small.

3.3 Catalytic activity comparison of the enzymes, ZIF-8 capsule and ZIF-8 capsule/PSF stereostructure

The as-prepared ZIF-8 capsule/PSF stereostructure may have great potential in glucose sensor fields. As an important indicator, the activity of the ZIF-8 capsule/PSF stereostructure for glucose

catalytic reduction was evaluated. With the GOx and HRP biocatalytic cascade system encapsulated, aerobic oxidation of glucose by GOx yields H_2O_2 and gluconic acid, and the generated H_2O_2 acts as a substrate for HRP, which catalyzes the oxidation of ABTS, generating a green-colored product (Fig. S1).

Table 1 shows the absorbance values of the enzymes ZIF-8 capsule and ZIF-8 capsule/PSF stereostructure with 4 mM glucose as the substrate at 450 nm using a microplate reader. For comparison, the ZIF-8 capsule powder used was 24% wt of ZIF-8 capsule/PSF stereostructure membrane, according to the EDS. The concentrations of GOx and HRP were 4% wt and 2.6% wt of the ZIF-8 capsule, respectively, according to the loading mass ratio as published by Chen[11]. The biocatalytic cascade in the ZIF-8 capsule showed an approximately 1-fold enhancement compared with the mixture of the two enzymes, and the ZIF-8 capsule/PSF stereostructure showed an approximately 0.2-fold enhancement compared with the ZIF-8 capsule. This difference is most likely because the stereostructure of PSF provides better dispersion and a larger reaction area. In addition, these values prove the existence of GOx and HRP in the ZIF-8 capsule and ZIF-8 capsule/PSF stereostructure.

Table 1. Time-dependent absorbance values of enzymes, ZIF-8 capsule and ZIF-8 capsule/PSF stereostructure at 450 nm with 4 mM glucose as substrate.

Time (min)	0	5	10	20	30
GOx/HRP	0.0470	0.1198	0.1684	0.3878	0.6122
ZIF-8 capsule	0.0484	0.1654	0.2523	0.6970	1.1287
ZIF-8 capsule/PSF	0.0481	0.1815	0.2768	0.8341	1.3920

To enlarge the linear range of the sensor, the ZIF-8 capsule/PSF stereostructure was modified twice with 5% Nafion. The glucose catalytic activity of the modified ZIF-8 capsule/PSF stereostructure was also evaluated spectrophotometrically with an o-dianisidine indicator in 0.05 M PBS (pH 6.5, room temperature, including 0.1 M KCl) incubated for 15 min at room temperature. According to Fig. 7, the ZIF-8 capsule/PSF stereostructure showed good linearity for the glucose reaction.

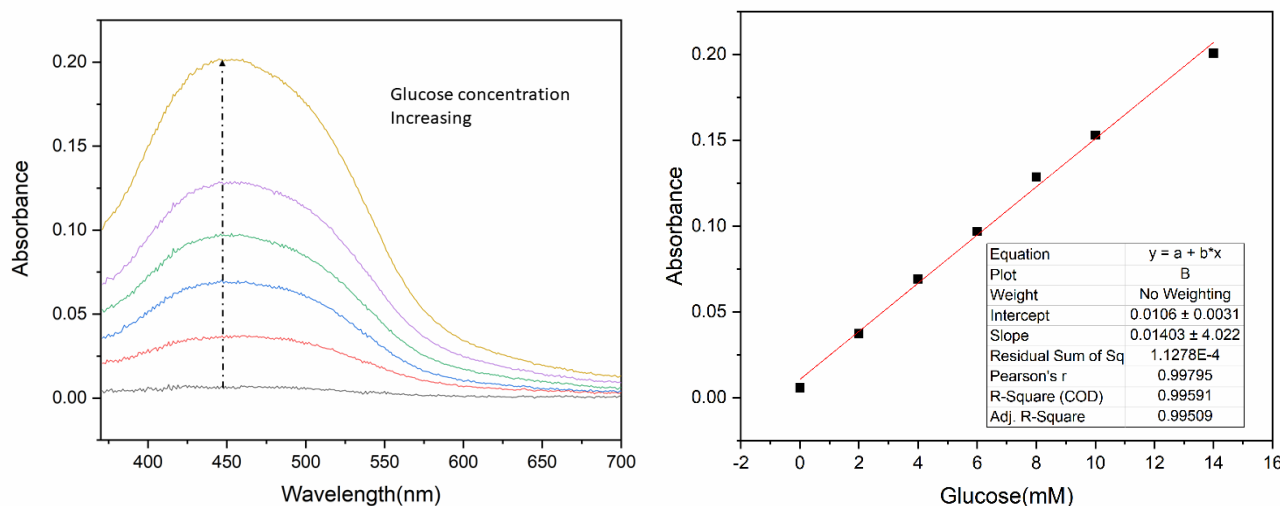


Figure 7. The figure A displays the responses of the ZIF-8 capsule/PSF stereostructure to glucose from 0 mM to 14 mM in 0.05 M PBS (pH=6.5, room temperature, including 0.1 M KCl). The figure B displays the corresponding calibration curve for glucose from 0 mM to 14 mM.

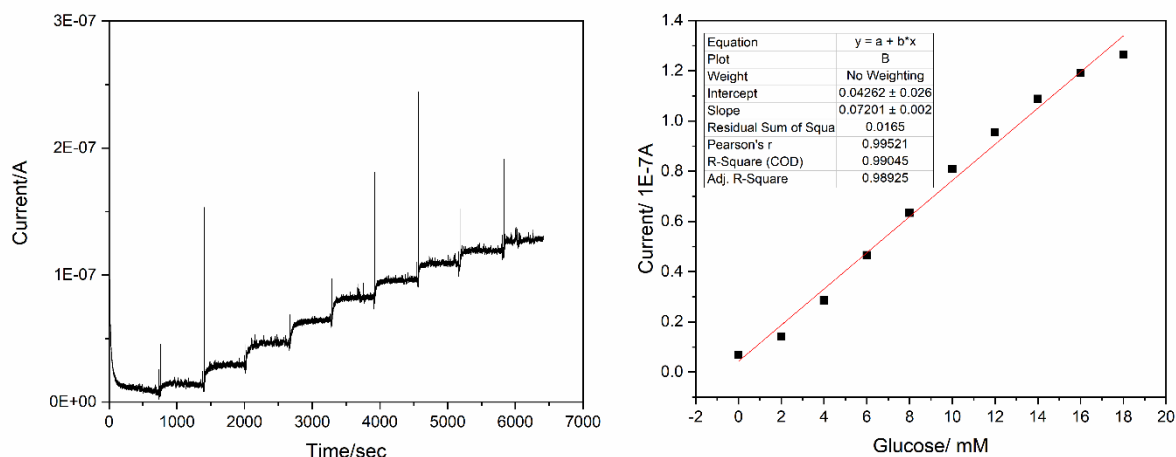


Figure 8. The figure A indicates the amperometric responses of the modified ZIF-8 capsule/PSF biosensor to successive injection of 2 mM glucose from 0 mM to 18 mM in 0.05 M PBS (pH=6.5, room temperature, including 0.1 M KCl) at 0.33 V. The figure B displays the corresponding calibration curve for glucose from 0 mM to 18 mM.

3.4 Electrocatalytic response to glucose on the ZIF-8 capsule/PSF sensor

As described in 2.4, ZIF-8 capsule/PSF glucose biosensors were fabricated to evaluate their analytical performance by amperometric measurements in 0.05 M PBS (pH 6.5, room temperature, including 0.1 M KCl) at an applied potential of 0.33 V (vs. Ag/AgCl) according to published studies[6, 28]. The amperometric response curve for the ZIF-8 capsule/PSF glucose biosensor with the successive addition of glucose (2.0 mM/step) is shown in Fig. 8A.

Table 2. Comparison of the performance of various glucose biosensors.

Modifiers	Sensitivity ($\mu\text{A mM}^{-1}$)	Linear range (mM)	Ref.
ZIF-8 capsule/PSF	0.07	2–18	This work
GO _x -HRP-PDMS	-	0.3-4.8	[29]
Pin-GO _x -HRP-PAA	1.44	0.05-1	[30]
Silica-GO _x -HRP-PAA	-	0-0.02	[31]
Carbon-GO _x -HRP	1.13	0.3-15	[32]
SnO ₂ fibers-GO _x -HRP	-	0.005-0.1	[33]
3D graphite-PB-GO _x -HRP	27.5	0.2-20	[34]
Paper-GO _x -HRP	-	0.1-2	[35]
ZIF-8/GO _x	-	0.1-1.7	[36]
Au-Fe ₃ O ₄ -GO _x	2.52	0.2-9	[37]

-, not mentioned; PDMS, polydimethylsiloxane; PAA, poly(acrylic acid); PB, Prussian blue.

Each injection was followed by stirring (200 rpm with a magnetic stirrer) for 3 min to homogenize the solution, which corresponds to the sharp decline and rebound at the beginning of each step in the curve. To verify the steady-state current for each step, each concentration was measured for

at least 10 min. As the glucose concentration increased, the response current of the biosensor increased up to 18 mM with a linear response. The corresponding calibration curve for the glucose response is shown in Fig. 8B. A linear relationship between the current and glucose concentration was obtained in the range of 0–18 mM, with an R^2 value of 0.99, according to equation $i/(\mu\text{A})=0.07 C_{\text{glucose}}(\text{mM})+0.04$. Compared with previously reported glucose biosensors (Table 1), the biosensor linear range is sufficient to meet the needs of diabetic patients.

As an enzyme-based biosensor, the ZIF-8 capsule/PSF glucose biosensor also followed Michaelis-Menten kinetics. The Michaelis-Menten constant, K_M , was calculated from the amperometric response curve and the visible absorption spectra with GraphPad prism 5.0 software; the values of K_M were found to be 10.14 mM and 12.7 mM, respectively.

3.4 Anti-interference test

AA and UA are common GOx-based glucose biosensor-interfering species in real blood samples[38]. The selectivity of the ZIF-8 capsule/PSF biosensor was evaluated by measuring amperometric responses due to an initial addition of 0.1 mM of each interfering species and then two 2.0 mM glucose injections (Fig. 9). The results proved that the ZIF-8 capsule/PSF biosensor had good anti-interferent abilities.

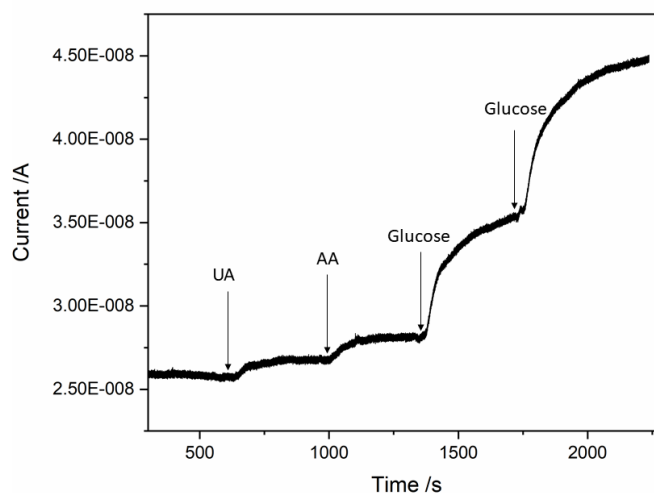


Figure 9. Amperometric response for 0.1 mM AA, 0.1 mM UA and 2.0 mM glucose on the ZIF-8 capsule/PSF biosensor in 0.1 M PBS (pH=6.5, including 0.1 M KCl). Applied potential: 0.33 V.

3.5 Human blood sample analyses

The electrochemical reaction of whole blood on ZIF-8 capsule/PSF biosensors was carried out as follows (Scheme, Fig. 10). (I) Dissolved oxygen in the blood penetrated into the PSF layer. (II) The blood glucose infiltrated into the ZIF-8 capsules with a consecutive series of enzymatic reactions. First, glucose was catalyzed by GOx inside the capsule to produce gluconolactone and H_2O_2 . As H_2O_2 was produced, the HRP inside the capsule immediately catalyzed the H_2O_2 to H_2O , and the catalysis also

caused the loss of electrons between the ZIF-8 capsule and the electrode. (III) The cells in the blood were blocked outside the PSF layer due to the PSF micropores.

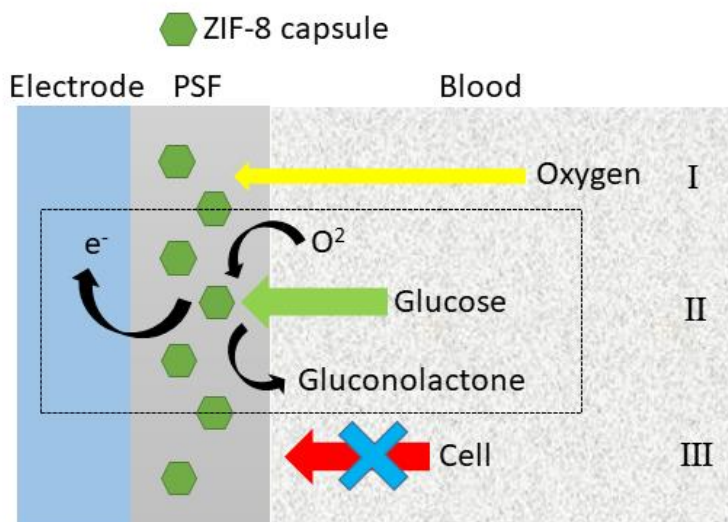


Figure 10. Schematic for the blood glucose electrochemical detection mechanism of ZIF-8 capsule/PSF biosensors.

To further assess the performance of the ZIF-8 capsule/PSF biosensors in whole blood samples, we measured the glucose concentrations in fresh human blood samples. All detected glucose concentrations of the blood samples were derived from the former standard curve and regression equation. A serum sample from one healthy volunteer was used for single point calibration. Bias values were determined by comparing the glucose concentration estimated by the ZIF-8 capsule/PSF biosensors and YSI 2300, which supports the whole blood test (Table 2). The results show that the error between the sensor and the YSI calibration value was less than 5% and the RSD was less than 3%, which indicates that the ZIF-8 capsule/PSF biosensor measurements have potential for whole blood glucose determination.

Table 2. Analysis results in serum samples ($N = 5$).

Sample No	Measured by YSI 2300 (mM)	Measured by ZIF-8 capsule/PSF biosensors (mM)	%RSD	Bias (mM)
1	5.75	5.54	2.39	-0.21
2	7.82	7.63	2.86	-0.19
3	8.30	8.09	1.11	-0.21

3.7 Repeatability tests

Furthermore, the repeatability of the modified ZIF-8 capsule/PSF biosensors towards the whole blood samples was tested. Whole blood samples from one healthy volunteer were used for the repeatability tests. ProClin 300 was added to the samples as preservative. The biosensors were repeatedly and carefully washed with ultrasonic cleaner for 5 min at room temperature after each test. The standard curve and regression equation were corrected by single point calibration before use. Fig. 11 shows the measurements of the samples during a 50-point repeatability test. After the 50-point repeatability test, the bias of the calculated blood glucose concentration and YSI calibration value was still less than 10%. This result exhibits the great repeatability of the modified ZIF-8 capsule/PSF biosensors.

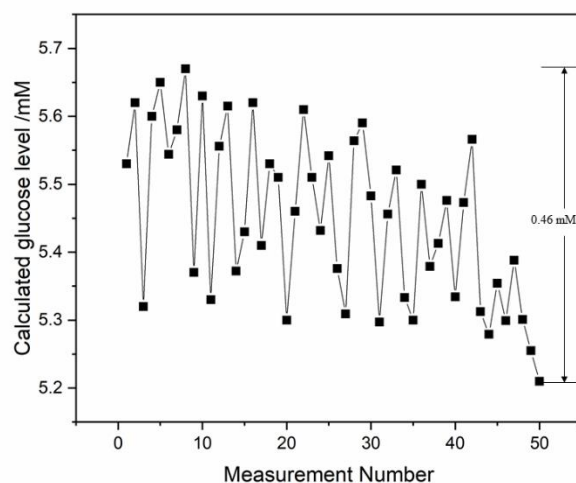


Figure 11. Measurements of one blood sample from a healthy volunteer during the 50-point repeatability test (pH=6.5, room temperature, including 0.1 M KCl) at 0.33 V.

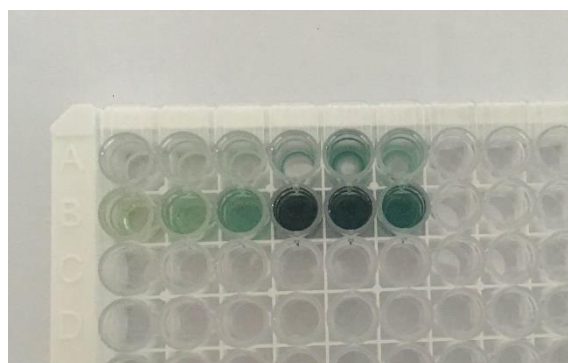


Figure S1. Time-dependent catalytic activity comparison of the enzymes, ZIF-8 capsule and ZIF-8 capsule/PSF stereostructure with ABTS indicator.

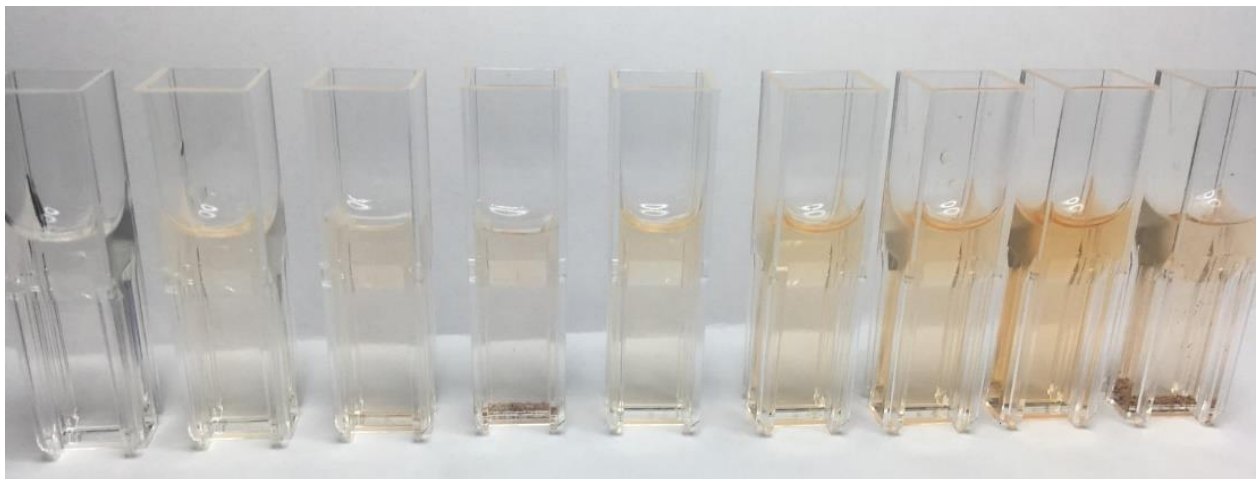


Figure S2. Glucose catalytic activity of modified ZIF-8 capsule/PSF stereostructure with the o-dianisidine indicator.

4. CONCLUSIONS

In conclusion, a novel ZIF-8 capsule/PSF stereostructure with GOx and HRP encapsulated in ZIF-8 was fabricated, and a glucose biosensor with good performance was developed based on this structure. Characterized by XRD, FT-IR, SEM and visible absorption spectra, the structure with uniform ZIF-8 capsules loaded exhibits higher sensitivity than does the ZIF-8 capsule powder, and 40 min of heating time was proven to be optimal for forming immobilized ZIF-8 capsules. The experiments revealed that the modified ZIF-8 capsule/PSF glucose biosensor exhibited a great linear range and good selectivity. Furthermore, the prepared sensor shows great performance in the repeatability testing of whole blood. The novel biocatalytic cascade in the ZIF-8 capsule/polysulfone stereostructure may have promising applications in whole blood monitoring.

ACKNOWLEDGMENTS

This research was supported by the Zhejiang Provincial Natural Science Foundation of China (Grant No. LY18H180009) and the Zhejiang Province Key R&D Project (Grant No. 2017C03029).

References

1. J. Wang, *Chemical reviews*, 108 (2008) 814.
2. D. Olczuk, R. Priefer, *Diabetes & Metabolic Syndrome: Clinical Research & Reviews*, 12 (2018) 181.
3. K.S. Park, S.A. Jin, K.H. Lee, J. Lee, I. Song, B.S. Lee, S. Kim, J. Sohn, C. Pak, G. Kim, *Int. J. Electrochem. Sci*, 11 (2016) 9295.
4. N.A.H.M. Nordin, S.M. Racha, T. Matsuura, N. Misdan, N.A.A. Sani, A.F. Ismail, A. Mustafa, *RSC Advances*, 5 (2015) 43110.

5. F. Cacho-Bailo, B. Seoane, C. Téllez, J. Coronas, *Journal of Membrane Science*, 464 (2014) 119.
6. S. Saha, S.K. Arya, S. Singh, B. Malhotra, K. Sreenivas, V. Gupta, *Materials Research Society Symposium Proceedings*, (2009) 45.
7. M.X. Wu, Y.W. Yang, *Advanced Materials*, 29 (2017) 1606.
8. S. Khatua, A. Kumar Bar, S. Konar, *Chemistry—A European Journal*, 22 (2016) 16277.
9. X. Lian, Y. Fang, E. Joseph, Q. Wang, J. Li, S. Banerjee, C. Lollar, X. Wang, H.C. Zhou, *Chemical Society Reviews*, 46 (2017) 3386.
10. J. Mehta, N. Bhardwaj, S.K. Bhardwaj, K.H. Kim, A. Deep, *Coordination Chemistry Reviews*, 322 (2016) 30.
11. W.H. Chen, M. Vázquez-González, A. Zoabi, R. Abu-Reziq, I. Willner, *Nature Catalysis*, 1 (2018) 689.
12. T.A. Golper, A.M.A. Saad, *Kidney international*, 30 (1986) 937.
13. A.S. Bargnoux, J.P. Cristol, I. Jaussent, L. Chalabi, P. Bories, J.J. Dion, P. Henri, M. Delage, A.M. Dupuy, S. Badiou, *Journal of Nephrology*, 26 (2013) 556.
14. R. Jin, Z. Bian, J. Li, M. Ding, L. Gao, *Dalton Transactions*, 42 (2013) 3936.
15. A.J. Brown, J. Johnson, M.E. Lydon, W.J. Koros, C.W. Jones, S. Nair, *Angewandte Chemie International Edition*, 51 (2012) 10615.
16. S. Ishaq, R. Tamime, M.R. Bilad, A.L. Khan, *Separation and Purification Technology*, 210 (2019) 442.
17. K. Eum, A. Rownaghi, D. Choi, R.R. Bhave, C.W. Jones, S. Nair, *Advanced Functional Materials*, 26 (2016) 5011.
18. J. Hou, P.D. Sutrisna, T. Wang, S. Gao, Q. Li, C. Zhou, S. Sun, H.C. Yang, F. Wei, M.T. Ruggiero, *ACS applied materials & interfaces*, 11 (2019) 5570.
19. M. Yang, Y. Liu, Y. Song, G. Zhao, H. Tan, Q. Zhang, F. Xu, *Int. J. Electrochem. Sci*, 12 (2017) 4428.
20. X. Mu, T. Bertron, C. Dunn, H. Qiao, J. Wu, Z. Zhao, C. Saldana, H. Qi, *Materials Horizons*, (2017) 442.
21. E.L.G. Medeiros, A.L. Braz, I.J. Porto, A. Menner, A. Bismarck, A.R. Boccaccini, W.C. Lepry, S.N. Nazhat, E.S. Medeiros, J.J. Blaker, *ACS Biomaterials Science & Engineering*, 2 (2016) 1442.
22. D. Ragab, H.G. Gomaa, R. Sabouni, M. Salem, M. Ren, J. Zhu, *Chemical Engineering Journal*, 300 (2016) 273.
23. Y. Zhang, S.J. Park, *Applied Catalysis B: Environmental*, 240 (2019) 92.
24. Y. Wang, C. Hou, Y. Zhang, F. He, M. Liu, X. Li, *Journal of Materials Chemistry B*, 4 (2016) 3695.
25. M. Jian, B. Liu, G. Zhang, R. Liu, X. Zhang, *Colloids and Surfaces A: Physicochemical and Engineering Aspects*, 465 (2015) 67.
26. Y. Cheng, J. Tao, G. Zhu, J.A. Soltis, B.A. Legg, E. Nakouzi, J.J. De Yoreo, M.L. Sushko, J. Liu, *Nanoscale*, (2018) 11907.
27. N.A.H.M. Nordin, A.F. Ismail, A. Mustafa, R.S. Murali, T. Matsuura, *RSC Advances*, 4 (2014) 52530.
28. Z. Yang, Y. Cao, J. Li, Z. Jian, Y. Zhang, X. Hu, *Analytica chimica acta*, 871 (2015) 35.
29. J. Tolós, Y. Moliner, C. Molins, P. Campíns, *Sensors and Actuators B: Chemical*, 258 (2018) 331.
30. E.C. Rama, A. García, M.T. Fernández, *Biosensors and Bioelectronics*, 88 (2017) 34.
31. Y. Zhao, Y. Wang, X. Zhang, R. Kong, L. Xia, F. Qu, *Talanta*, 155 (2016) 265.
32. O. Gutiérrez, E. Costa Rama, A. García, M.T. Abedul, *J. Biosens. Bioelectron.*, 93 (2017) 40.
33. S. Alim, A.K.M. Kafi, J. Rajan, M.M. Yusoff, *International Journal of Biological Macromolecules*, 123 (2019) 1028.
34. Y. Zhang, B. Huang, F. Yu, Q. Yuan, M. Gu, J. Ji, Y. Zhang, Y. Li, *Microchimica Acta*, 185 (2018) 86.
35. B.H. Kang, M. Park, K.H. Jeong, *BioChip Journal*, 11 (2017) 294.
36. Q. Wang, X. Zhang, L. Huang, Z. Zhang, S. Dong, *Angewandte Chemie International Edition*, 56

(2017) 16082.

37. A. Samphao, P. Butmee, J. Jitcharoen, L. Švorc, G. Raber, K. Kalcher, *Talanta*, 142 (2015) 35.

38. S. Husmann, E. Nossol, A.J.G. Zarbin, *Sensors and Actuators B: Chemical*, 192 (2014) 782.

© 2019 The Authors. Published by ESG (www.electrochemsci.org). This article is an open access article distributed under the terms and conditions of the Creative Commons Attribution license (<http://creativecommons.org/licenses/by/4.0/>).